Electronic Supporting Information

Exchange modified DOSY Experiments. The use of Chiral Solvating Agents and Lanthanide Shift Reagents as matrices.

(Submitted to New Journal of Chemistry)

Gábor Szalontai

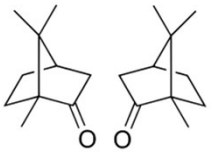

(L1)

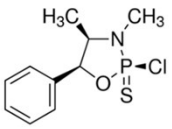

(L2)

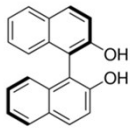

CSA: (S)-BINOL (288 Da)

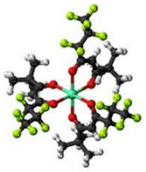

LS reagent: Eu(fod)$_3$ (1038 Da)

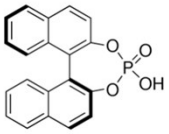

(L3)

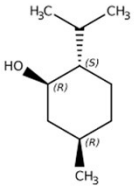

(L4)

Content

1. Theory and methods

1.1 Rotational diffusion: information obtainable from ^{1}H T_1 relaxation studies.

It is known that T_1 relaxation time constants provide information also on the rotational diffusion coefficient, $\boldsymbol{D^r}$ of a molecule.[2] Relaxation measurements are more sensitive to motions occurring in the *picosecond* to *nanosecond* time scales, i.e. to extremely high frequencies compared to translational diffusion. $\boldsymbol{D^r}$, like the translational diffusion coefficients, depends not only on the reciprocal third power of the molecular size (~ 1/hydrodynamic radius, $\mathbf{a^3}$**)** and shape of the molecules but also on the temperature, composition, and viscosity of the solvent used.[1,2,5] This is because the molecular rotational correlation time, $\boldsymbol{\tau_c}$ is reciprocally related to $\boldsymbol{D^r}$.

$$\boldsymbol{D^r = k_B T/8\pi\eta_o a^3} \quad \boldsymbol{\tau_c = 4\pi a^3\eta_o/3kT} \quad \boldsymbol{D^r = 1/3\tau_c}$$

However, to make good use of these dependencies there are, like the $\boldsymbol{D^t}$ case, a number of assumptions which must be justified.[2] In addition to those already mentioned the relaxation mechanisms also needs to be known, inter- and intramolecular contributions must be separated.

1.2 Distances: When studying the effect of exchange the absolute distance, **z** a molecule can travel is also of interest. Its square, $\mathbf{z^2}$ is directly proportional to the product of the diffusion coefficient and the duration, **t**.

$$\mathbf{z^2} = 2*\boldsymbol{D^t}*t^{27}$$

[27] J. Crank, *Mathematics of Diffusion*, Oxford Univ. Press, New York, 1975.

1.3 Paramagnetism[18], lanthanides[33]: The key to the lanthanide induced shift (LIS) and relaxation enhancement (PRE) phenomena is the formation of a complex between a nucleophile and a coordinatively unsaturated lanthanide chelate. The lifetime of the complexes are short, consequently the induced shifts (LIS = δ_{obs}- $\delta_{diamag.}$) are normally not available from the spectra. Concerning the structure of adducts these complexes readily expand their coordination number beyond six.[28] They associate with a wide variety of basic ligands, may form hydrates, and self-associated oligomers. The average metal – coordinating atom (O, N) distance is about 3 Å, this distance is sufficiently short to induce substantial paramagnetic shifts. In Eu^{3+} complexes for protons the predominant magnetic interaction is a dipolar type effect (pseudocontact shift). The f-blocks elements (the non-paired electrons) are not bond-forming, therefore ligand field effects are less pronounced, and the point charge approximation is valid.[19] Fortunately, the shifts are accompanied only by little line broadenings. The relaxation effect decreases with an $\mathbf{r^{-6}}$ dependence where **r** is the distance between the paramagnetic centre and the nucleus whose signals is being observed. Concerning the solvents their effect on the association can be significant, that is why "neutral" solvents such as CCl_4 or $CDCl_3$, which do not hinder the complex formation, are preferably used.

Of the numerous lanthanide complexes the $Eu(fod)_3$ proved to be one of the most effective[33], though, one must add, not in all cases.

1.4 $\boldsymbol{D^t}$ calculation using the Stokes-Einstein Gierer-Wirtz Estimation (SEGWE) equation developed by the Morris group[25,26]:

$$D = \frac{k_B T\left(\frac{3\alpha}{2} + \frac{1}{1+\alpha}\right)}{6\pi\eta^3\sqrt{\frac{3MW}{4\pi\rho_{eff}N_A}}} \qquad \alpha = \frac{r_S}{r} = \sqrt[3]{\frac{MW_S}{MW}}$$

where ρ_{eff} = effective molecular density, $\mathbf{r_S}$ and **r** are the hydrodynamic radius of the solvent and the ligand, respectively. $\mathbf{MW_s}$ and **MW** are the molecular masses of the solvent and the ligand, respectively. η = solvent viscosity. The other symbols have their usual meanings.

2. Matrix: CSA

2.1 Tormena's paper: (Chem.Commun. 2019, 55, 8611.)

$\mathbf{D^t}$ resolution improvement by adding CSAs: Several illustrative examples of the improved D resolution upon addition of a CSA has been published in the literature, e.g. Salome and Tormena reported different camphor $\mathbf{D^t}$ coefficients for the two diastereomers (structures **8, 9** in their paper) in *(S)*-BINOL matrix (doublet: 1.518, 1.525 (S) and doublet: 1.501, 1.503 (R)- 10^{-9} m^2/s **($\Delta D \sim 0.02 * 10^{-9}$ m^2/s)** in 3 mm tube, 25 °C, non-spinning, 300 μL, 11.7 T).
In fact under similar conditions (3 mm tube, non-spinning sample, 298 K, non-regulated, 400 l/h cooling air flow, without lock, and 9.4 T static field) we could not observe D resolution between the two binol – camphor diastereomers (Δ = 50 -100 ms, Echo numbers = 16, without zero-filling!).

2.2 DOSY (*R,S*)-oxazaphos – (*S*)-BINOL mixture

(*S*)-BINOL - (*R,S*)-oxazaphospholidine-2-sulphide derivative (**L2**): a pair of similar agent and ligand sizes (288 Da *vs*. 245 Da, $\mathbf{f_{mw}} \sim 1.2$), since self-aggregation of the ligands cannot be excluded the molar ratio dependence was also looked at.

^{1}H NMR: At low agent concentration ($\mathbf{f_{molar}} \sim 0.3$) only the multiplet at 3.8 ppm (CH_3-C**H**-N) shows the expected *enantiodifferentiation* effect (see Figure 5. below), nevertheless adduct with its roughly doubled molecular weight must, at least temporary, exist. At higher *(S)*-BINOL concentration several other ligand resonance also exhibited splittings (not shown).

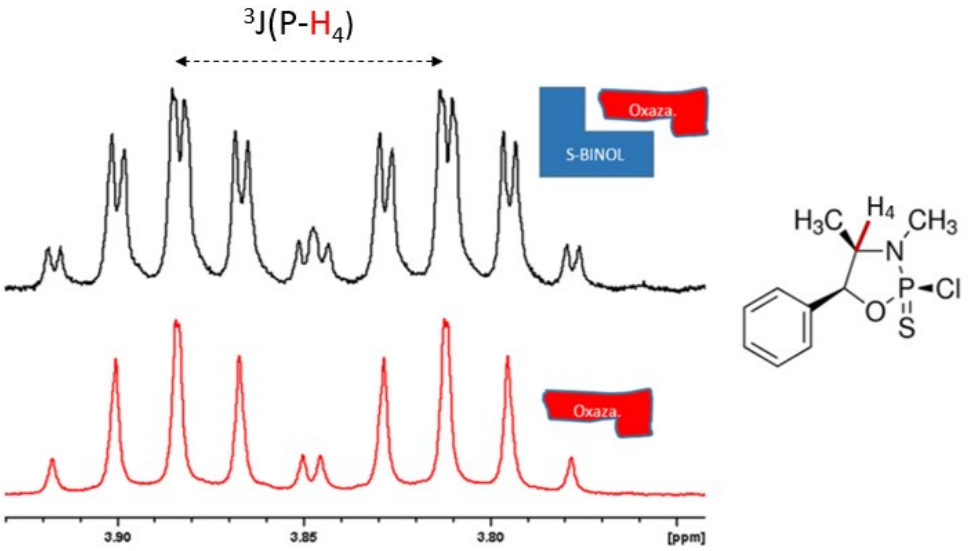

Figure S1. Comparison of ^{1}H NMR spectra of the free ligand (bottom) and a mixture of *(S)*-BINOL and (*R,S*)-oxazaphos (**L2**), $\mathbf{f_{molar}}$ = 1.06 recorded in 0.4 ml $CDCl_3$ (top). Expansion, H_4 (CH_3-**C**H-N-P) proton only, $^{3}J(^{31}P\text{-}^{1}H)$ = 28.6 Hz.

DOSY experiments: two resolved signals were observed in the diffusion dimension. In the mixture $\mathbf{f_{molar}}$ ratio dependence of the $\boldsymbol{D^t}$ values in the 0.6 – 1.6 region could not be justified. In the $\mathbf{f_{molar}}$ range of the mixture the obtained $\boldsymbol{D^t}$ values are identical within the experimental error. the data do not support ligand self-aggregation. In $CDCl_3$ the SEGWE estimates are high, perhaps due to the low ligand/solvent hydrodynamic radius ratio (the ligand is not large enough). Notice, that at all agent concentrations the apparent oxazaphos $\boldsymbol{D^t}$ is approaching that of the free ligand (L2).

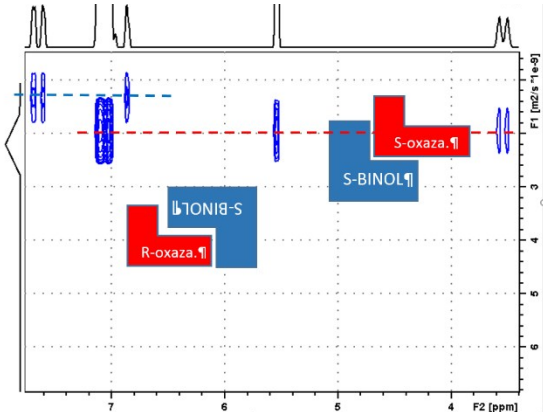

Fig. S2. ^{1}H DOSY of the (*R,S*)-oxazaphospholidone-2-sulphide (245 Da) - (*S*)-BINOL (288 Da) mixture recorded in $CDCl_3$ solution, 300 K (regulated), $\mathbf{f_{molar}}$ **~ 1.06**.

2.3 Relaxation in CSA mixtures: rotational diffusion

Selected ^{1}H T_1 constants observed in the mixture in $CDCl_3$ at RT:

Free oxazaphospholidine-sulfide
H 5.87 ppm (3.08s)
H_4 3.86 ppm (2.36s)
H 2.92 ppm (2.06s)
H 0.9 ppm (1.15s)

Oxazaphospholidine-sulfide – (*S*)-BINOL mixture:
7.95 ppm (2.07s)
7.91 ppm (2.2s)
7.18 ppm (2.45s)

oxaza in mixture
5.86 ppm (2.88s)
H_4 3.86 ppm (2.36s)
2.96 ppm (1.9s)
0.94 ppm (1.06s)

Table S1.

$\mathbf{f_{molar}}$ BINOL/oxazaphos.	**0.6**	**1.20**	**1.6**	Predictions (SEGWE)[26]
Mixture***:*** BINOL (apparent)	0.91	1.02	0.87	
***D*^{t}** free BINOL (288 Da)	0.91 (5 mg/0.3 ml) 0.83 (15 mg/0.3 ml)			1.231
Mixture: oxazaphos (apparent)	1.06	1.10	1.00	
***D*^{t}** free oxazaphos (**L2**) (245 Da)	1.14 (5 mg/0.3 ml) 1.21 (15 mg/0.3 ml)			1.330
Adduct (288 + 245 Da)	n.o.			0.908
The values are given *10^{-9} m^2/s, exp. error = +/- 0.1, 300 K, $CDCl_3$				

Relaxation: Selected ^{1}H T_1 constants measured in an $\mathbf{f_{molar}}$ **~ 1.06** mixture in $CDCl_3$ at room temperature can be found in ESI material (point 1.3). They are tendentiously shorter by about 10 % in the mixture, this can be explained by temporary adduct formation (somewhat slower rotational diffusion), however, even the higher viscosity of the mixture can be responsible for this. Conclusion: slow exchange both in the diffusion and chemical shift dimensions.

2.4 $^{31}P\{^1H\}$ and $^{13}C\{^1H\}$ spectra:

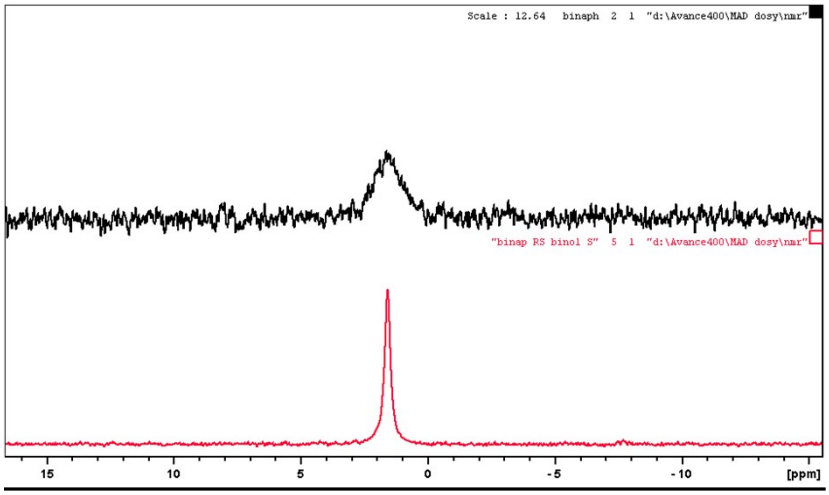

Fig. S3. ^{31}P $\{^{1}H\}$ NMR spectrum of 8 mg (+) and 9 mg (-) binaphthalene –diyl-hydrogen-phosphate enantiomers + 40 mg (*S*)-BINOL mixture (bottom), (molar ratio ~ 3:1, weight ratio 40:17) recorded in ethanol-d_6. (Top) free binaphthalene (*R,S)* recorded in $CDCl_3$/ethanol-d_6.

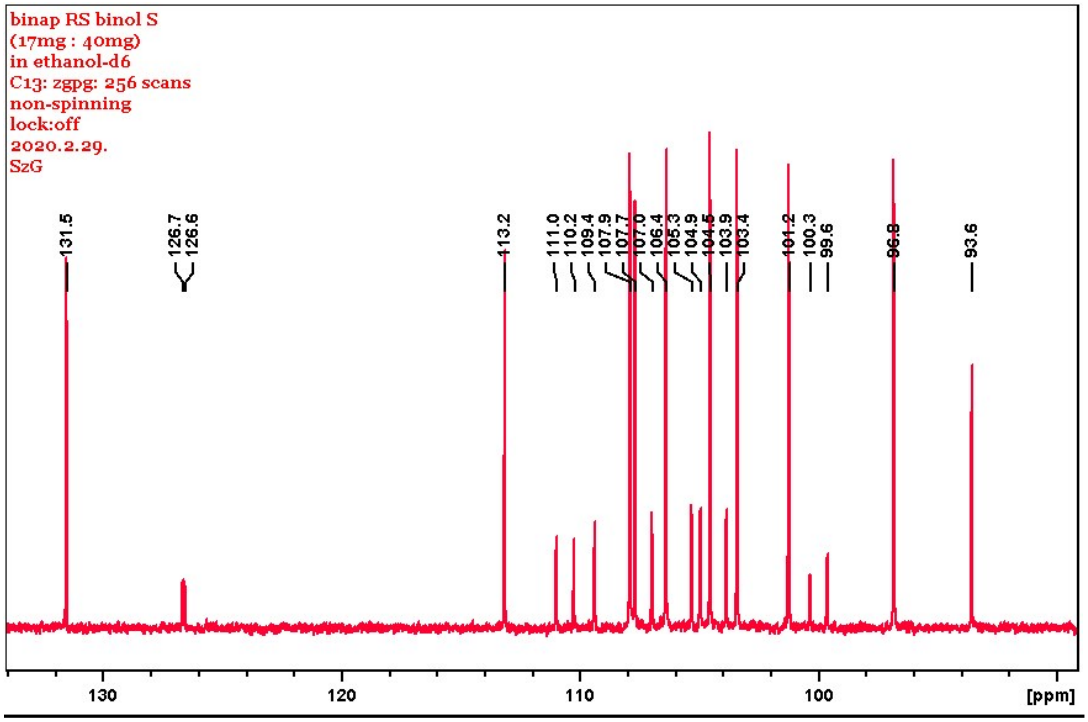

Fig. S4. $^{13}C\{^{1}H\}$ spectrum of the same mixture (8 mg (+) and 9 mg (-) binaphthalene –diyl-hydrogen-phosphate enantiomers + 40 mg (*S*)-BINOL recorded in ethanol-d_6.

Unlike the free binap enantiomeric mixture (see ^{31}P spectrum in Fig. S3) recorded in a mixture of $CDCl_3$ /ethanol the ^{31}P signal of (*R,S)*-binaphthalene– (*S*)-BINOL mixture is relatively narrow (~ 30 Hz). At the same time the ^{13}C $\{^{1}H\}$ spectrum (notice the narrow lines)

has 10 signals both for the (*S*)-BINOL and binaphthalene molecules, i.e. highly symmetric time averaged structures can be assumed.

2.5 A ternary mixture: (R,S)-oxazaphospholidine-sulfide (ligand) – (**CSA**) (*S*)-BINOL – (**LSR**) Eu(fod)$_3$ (agents)

^{1}H NMR: Below we compare the simultaneous effect of the chiral solvating agent (CSA) (*S*)-BINOL and the achiral LSR agent Eu(fod)$_3$ on the ^{1}H spectrum of a mixture of R and S forms of oxazaphospholidine-2-sulfide. Note that this molecule, possessing several functional groups, is capable to form weaker or stronger intermolecular bindings.

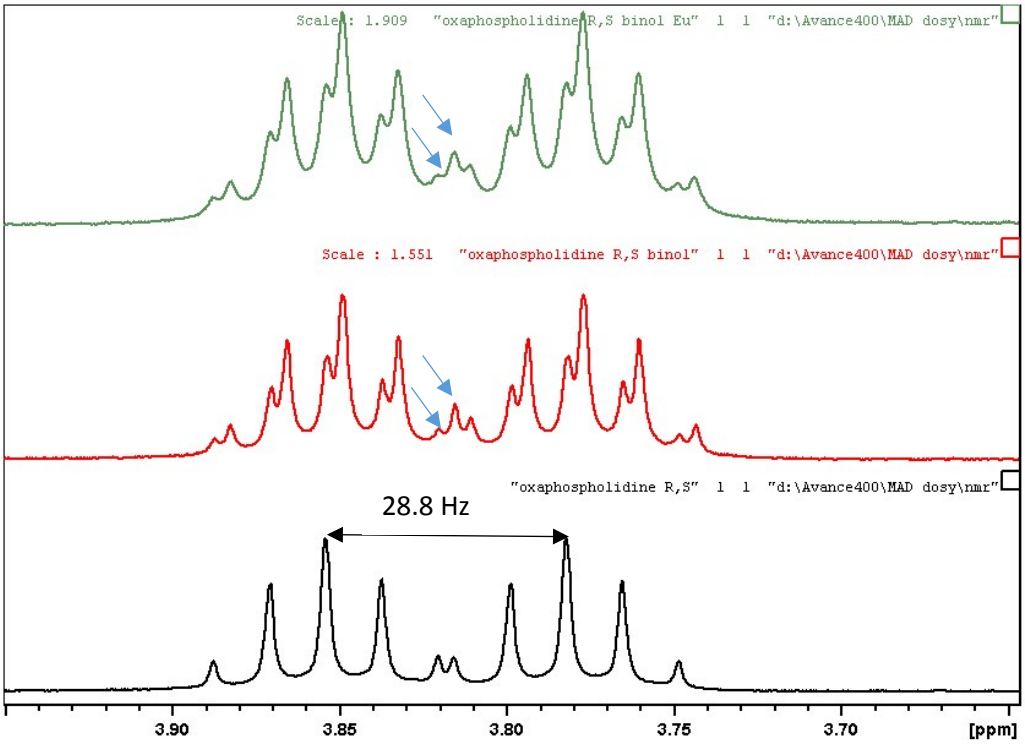

Fig. S5. ^{1}H NMR: A ternary mixture: the effect of sequential addition of (26 mg = 90 microM) (288D) (*S*)-BINOL middle) and Eu(fod)$_3$ (58 mg=56 microM/l top) to the ^{1}H NMR spectrum of an oxazaphospholidine-2-sulfide mixture (245 Da) (+) 7 mg **(28 micromol**) and (-) 13 mg (53 microM/l) in 0.45 mL = $CDCl_3$ (5.7 mol, bottom) (Note the extreme excess of solvent molecules by a factor of about 10^3!).

Notice that, once again, only one signal at 3.81 ppm (CH_3-$H_{4R,S}$-N) is split upon addition of the chiral solvating agent (*S*)-BINOL, all other signal remained unchanged! The observed intensity ratio of the two enantiomers agrees with the expectation. At the same time there are,

though not significant, changes of the (*S*)-BINOL signals confirming that short-lived adducts were possible forming among the binol and the oxazaphospholidine-2-sulfide.

3. LSR matrix

At the same time the LS agent $Eu(fod)_3$, used in a twofold excess (for the (+) form) and in 1:1 molar ratio with the (-) form, does not induce measurable paramagnetic shifts of the oxazaphospholidine-2-sulfide signals.

3.1 $Eu(fod)_3$ – oxazaphos mixture, VT spectra in $CDCl_3$, $\mathbf{f_{molar}}$ = 18.4 : 8.8 ~ 2.1

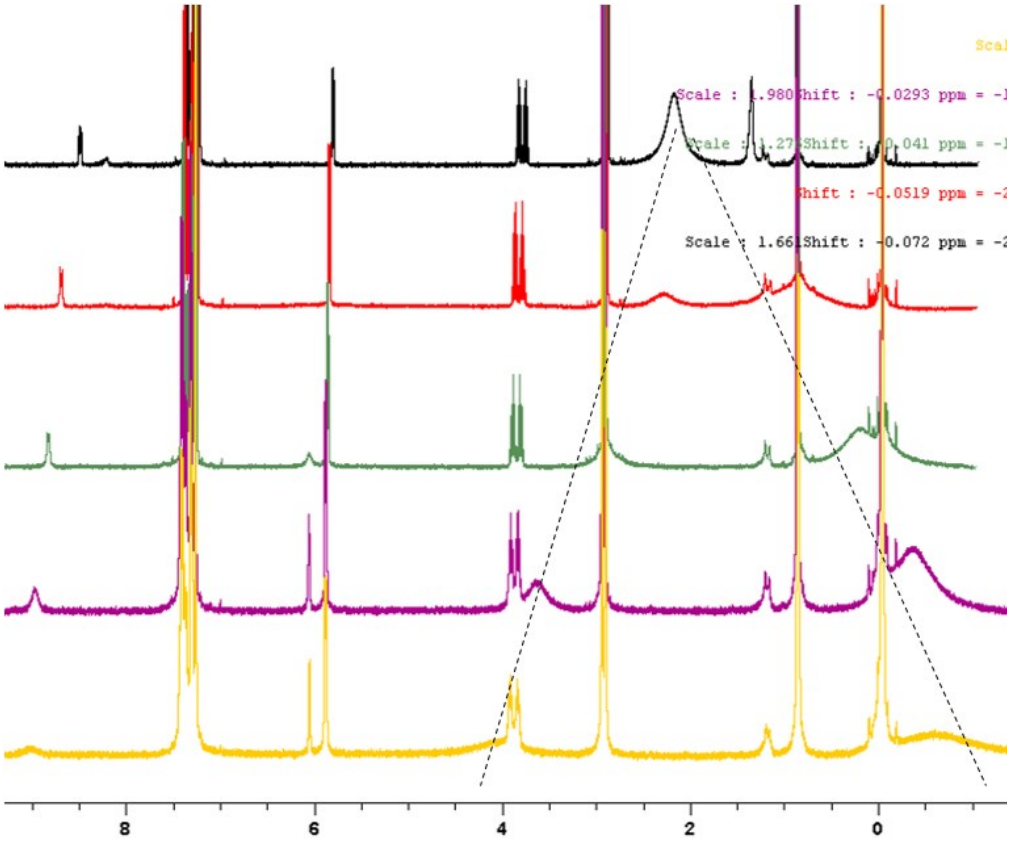

Fig. S6. ^1H spectra: T = 223, 233, 253, 273 and 323 K. While the oxazaphos signals do not change upon cooling the broad singlet of the $Eu(fod)_3$ methyl broadens and is split. The reason is unclear, dimer formation is suspected.

Results of (R,S)-oxazaphospholidine-sulfide – (*S*)-BINOL – (**LSR**) $Eu(fod)_3$ ternary mixture experiment were confirmed by study of binary mixtures (see below) as well, which indicated

that none of the oxazaphospholidine enantiomers forms adduct with the Eu^{3+} complex (ions), even in the absense of (S)-BINOL. Agent-LIS reagent-ligand mass ratio = 288:1037:245.

4. ^{19}F (proton coupled) spectra: 1D ^{19}F NMR spectroscopy of $Eu(fod)_3$ dopped systems. The ^{19}F nucleus (I=1/2), due to its high sensitivity and large chemical shift range [C. Tormena, *Progress in NMR* Spec. 2016, 96, 73.] is very attractive for many applications. Often, it produces larger chemical shift difference values in comparison with ^{1}H and thus makes possible more accurate diffusion coefficient values. In case of F containing agents or ligands it is often the method of choice. It turned also out that exchange processes and the underlying chemistry can easily be followed by looking at the ^{19}F spectra of binary and ternary systems. In this respect the $Eu(fod)_3$ complex is of special interest since frequently good use of the paramagnetic shift and relaxation effect can be made. In the following a few examples of 1D ^{19}F exchange spectroscopy will be shown.

4.1 Binary system (1). Chiral solvating agents: the effect of (*S*)-BINOL
Substrate: methoxy-α-trifluoromethylphenyl-acetic acid, an *R,S*-mixture.

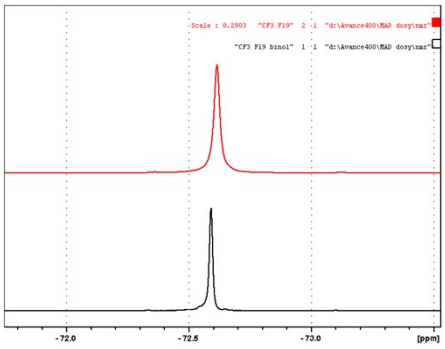

Fig. S7. ^{19}F (proton coupled) NMR spectrum ($CDCl_3$) of (*R,S*)-**methoxy-α-trifluoromethylphenyl-acetic acid** ($C_{10}H_9O_3F_3$ = 214 Da), a 3 mg + 6 mg mixture of *S* and *R* enantiomers = 4.2 micromol (bottom) and after addition of 14 mg (*S*)-BINOL = 4.8 micromol (top).

As seen the substrate's CF_3 signal (-72.2 ppm), apart from some line broadening, does not change much (-72.6 ppm) upon addition of 14 mg (*S*)-BINOL (top), i.e. it does not form long-lived adduct with the (*S*)-BINOL). **f = 0.875.**

4.2 Binary system (2). Paramagnetic lanthanide shift reagents (LSR): $Eu(fod)_3$

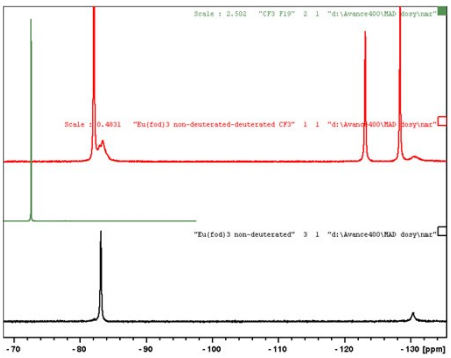

Fig. S8. ^{19}F-^{1}H NMR spectra: pure of $Eu(fod)_3$ in $CDCl_3$ (bottom), pure ^{19}F NMR spectrum of **methoxy-α-trifluoromethylphenyl-acetic acid** in $CDCl_3$ (a 3 mg + 6 mg mixture of *R* and *S* enantiomers) (middle), and the same sample after addition of 19 mg $Eu(fod)_3$ (top).

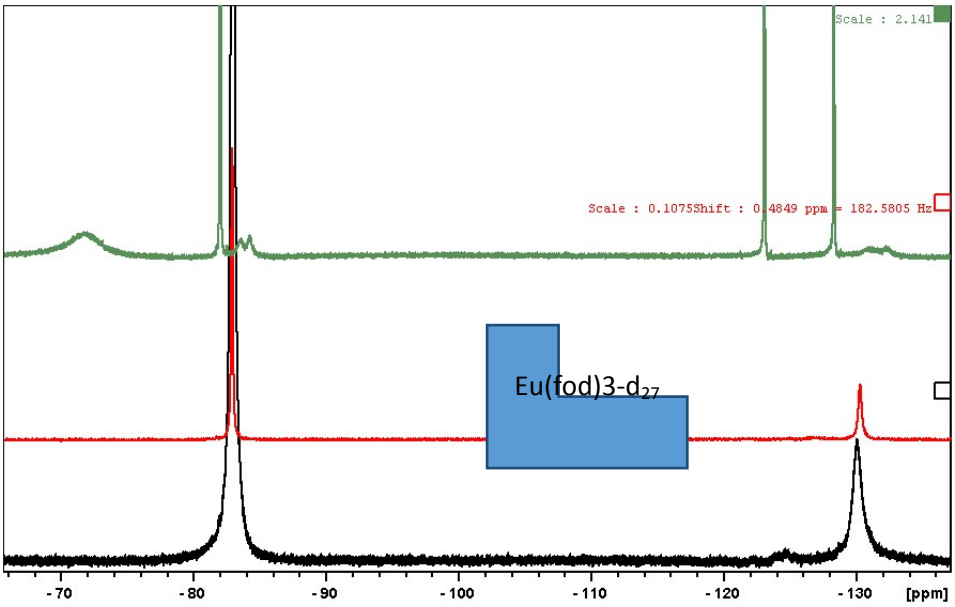

Fig. S9. ^{19}F NMR spectra: (bottom) 19 mg $Eu(fod)_3$ + oxazaphospholidine-2-sulfide (*R,S*) (8 mg *R*, 6 mg *S*) + CH_2Cl_2 (LSR agent – ligand ratio (0.32 :1)) in $CDCl_3$, (middle) 10-12 mg $Eu(fod)_3$ + CH_2Cl_2 and (top) ternary mixture: **methoxy-α-trifluoromethyl-phenyl-acetic acid** ligand - (S)-BINOL - $Eu(fod)_3$.

Spectra of the intact $Eu(fod)_3$ complex (Fig. S9. middle) show less than expected signals perhaps due to the enhanced paramagnetic relaxation contribution (PRE) of the Eu^{3+} ion. Signal of the CF_2 group nearest to the paramagnetic centre broadens beyond detection.

The Eu^{3+} ions with $4f^6$ electron orbital configurations may have relatively long electron relaxation time and thus cause substantial paramagnetic line broadening on the signals of nearby atoms. Perhaps that is why we do not see all fluorine signals in case of the free Eu(fod)3 (Fig.S9) or in case of the oxazaphospholidine – $Eu(fod)_3$ mixture where the

oxazaphospholidine ligand, for some reason and in line with the ^{1}H observation (Fig.), does not coordinate to the complex. This phenomenone, upon addition of a Lewis base 4-heptanone to $Eu(fod)_3$, has been observed very early and was explained by stereochechemical changes and oligomer formation[19] [C.S. Springer, A. H. Bruder, S. R. Tanny, M. Pickering, H. A. Rockefeller. p. 283. in E. Sievers (Ed.) *Nuclear Magnetic Resonance Shift Reagents*, Academic Press, Inc. London, 1973].
No doubt the presence of a ligand (substrate) molecule, depending on its coordination ability, may cause significant spectral changes. Examples are given below.

4.3 $Eu(fod)_3$ stability with carboxylic acids: upon addition of the carboxylic acid derivative ((*R,S*)-**methoxy-α-trifluoromethylphenyl-acetic acid**) the spectrum changes dramatically (Fig. and Fig, top). We assume that the substrate replaces the **fod** molecules or at least one of them in the coordination sphere of the Eu^{3+} ion. By taking up a proton from the carboxylic group one coordinated **fod** leaves the coordination sphere and transforms immedietly to diamagnetic **Hfod** [see Sievers]. Perhaps this is why all fluorine signals of the **fod**, being freed from the relaxation effect of the close Eu^{3+} ion, become also visible (see Figs).

e.g. $Eu(fod)_3 + R\text{-}COOH \leftrightarrow RCOO\text{-}Eu(fod)_2 + Hfod$

If so, the broad signals, low-frequency to the sharp ones, can be assigned to forms in which only one or two **fod** has been replaced by substrate (in case of an acidic derivative the shorter biting distance of the $–COO^-$ group can be more advantagous for the coordination). Note that others speculated on the presence of oligomers $(Eu(fod)_3)_{\mathbf{n}}$ or of $H(Eu(fod)_4)$ species or even monomer –dimer- oligomer equilibria in solution. [S. Dyer, J. A. S. Cunningham, J. J. Brooks, R. E. Sievers, R. E. Rondeau, in E. Sievers (Ed.) *Nuclear Magnetic Resonance Shift Reagents*, p. 21- 52. Academic Press, Inc. London, 1973.]

4.4 Further examples: Summary of changes of the Eu(fod)$_3$ ^{19}F NMR spectrum upon ligand coordination equilibria.

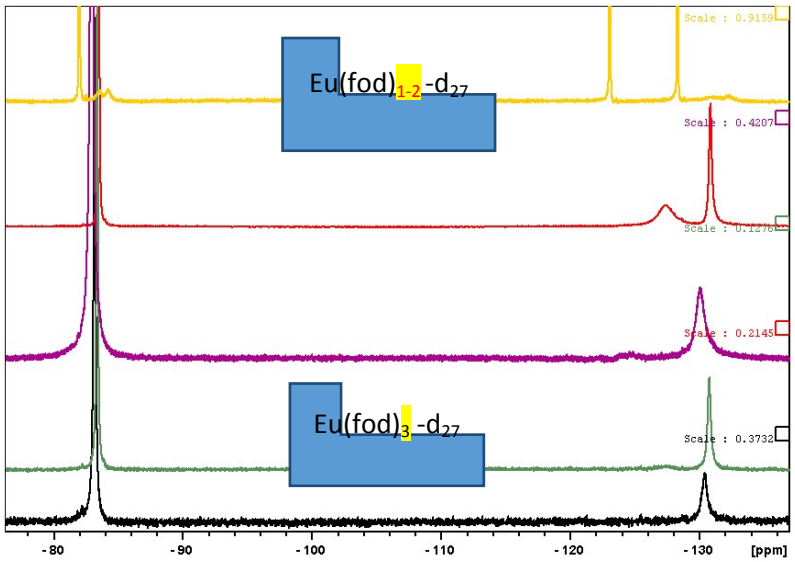

Fig. S10.^{19}F NMR spectra of Eu(fod)$_3$ recorded in 0.4 ml $CDCl_3$: black and green (bottom) in $CDCl_3$ and in $CDCl_3$ + 30 µL CH_2Cl_2. Purple: a mixture 19 mg Eu(fod)$_3$ + (8 mg *R*, 6 mg *S*)-oxazaphospholidine. Red: a mixture 19 mg Eu(fod)$_3$ + camphor (mg). Yellow: methoxy-α-trifluoromethyl-phenyl-acetic acid -(*S*)-BINOL -Eu(fod)$_3$ ternary mixture (top).

Oxazaphospholidine (Fig. 3rd from bottom): while the chemical shifts do not change, all ^{19}F signals, even that of the remote CF_3 group, are broad, an equilibrium strongly shifted toward the Eu(fod)$_3$ complex is suspected! Shifts of the remote protons are not informative in this respect.

Racemic-camphor (Fig. 4nd from bottom): all ^{19}F signals are clearly seen, modest selective broadenings are observed, this, in line with the paramagnetic shifts observed in the ^{1}H spectrum, can be explained by an Eu-fod ↔ Eu-camphor equilibrium with significantly longer lifetime (in comparison with the oxazaphospholidine case) of the Eu-camphor adduct!

Methoxy-α-trifluoromethyl-phenyl-acetic acid -(*S*)-BINOL -Eu(fod)$_3$ ternary mixture (Fig. 5th from bottom): formation of Hfod is likely, on time average at least one **CF_3** ligand is bond to the Eu^{2+} ion. The broadened signals at about – 83 and -135 ppm can be explained by the presence of two non-identical fod ligands. Note that due to the coordination of a methoxy-α-trifluoromethylphenyl-acetic acid ligand the symmetry of the complex vanishes.

Binaphthalene (*R,S*) mixture (348 Da) in methanol + (*S*)-BINOL: CSA effect is not observed!

4.5 The utility of ^{2}H DOSY for the same purpose has been pointed out recently by J. Guang et al. using calibration mixtures.[9] Later on the use of a universal calibration curve for each solvent (log (**Dη**) vs. log(**MW**)) has been suggested for polymers.[24]

^{2}H calibration mixture (listed in the figure) + Eu(fod)$_3$-d$_{27}$:

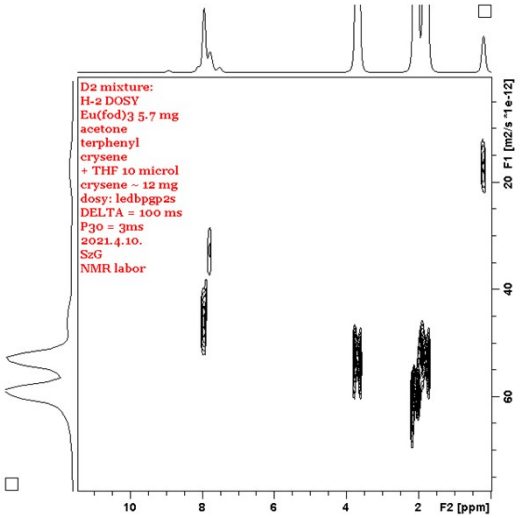

Fig. S11. ^{2}H DOSY map (ledbpgps2, 61.3 MHz, 300 K.

References from the main text

Literature

1 H. Barjat, G. A. Morris, S. Smart, A. G. Swanson and S. C. R. Williams, *J. Magn. Reson*. B., 1995, 108, 170.

2 W. S. Price, *Concepts in Magnetic Resonance* Part I, 1997, 9, 299.

3 A. R. Waldeck, P. W. Kuchel, A. J. Lennon and B. E. Capman, *Prog. Nucl. Magn. Res. Spectroscopy*, 1997, 30, 39.

4 C. S. Johnson Jr., *J. Magn. Reson*. A, 1993, 102, 214.

5 C. S. Johnson, *Prog. NMR Spectrosc*., 1999, 34, 203.

6 W. S. Price, *Concepts in Magnetic Resonance* Part II, 1998, 10, 197.

7 B. Antalek, *Concepts in Magnetic Resonance* Part A. 2007, 30, 219.

8 G. Dal Poggetto, V. U. Antunes, M. Nilsson, G. A. Morris and C. F. Tormena, *Magn. Reson. Chem.,* 2017, 55, 323.

9 J. Guang, R. Hopson and P. G. Williard, *J. Org. Chem*., 2015, 80, 9102.

10 I. J. Day *Progress in NMR Spectrosc*., 2020, 116, 1.

11 S. Caldarelli, in *Annual Reports on NMR Spectroscopy*, Elsevier Ltd, 2011, 73, Chapter 5, p. 159.

12 N. V. Gramosa, N. M. S. P. Ricardo, R. W. Adams, G. A. Morris and M. Nilsson, *Magn. Reson. Chem.,* 2016, 54, 815.

13 R. Evans and I. J. Day, *RSC Advances*, 2016, 6, 47010.

14 C. T. W. Moonen, P. van Gelderen, Q. W. Vuister and P. C. M. van Zilj, *J. Magn. Reson*., 1992, 97, 419.

15 E. J. Cabrita, S. Berger, *Magn. Reson. Chem.,* 2002, 40, S122.

16 C. C. Hinckley, *J. Am. Chem. Soc.,* 1969, 91, 5160.

17 C. Kutal in *Nuclear Magnetic Resonance Shift Reagents*, ed. E. Sievers, Academic Press, Inc. London, 1973. p. 87.

18 F. Balzano, G. Uccello-Barretta and F. Aiello, in *Chiral Analysis by NMR,* Elsevier B. V., Amsterdam, 2018. Chapter 9, p. 367.

19 C. S. Springer, A. H. Bruder, S. R. Tanny, M. Pickering and H. A. Rockefeller, in *Nuclear Magnetic Resonance Shift Reagents*, ed. E. Sievers, Academic Press, Inc. London, 1973. p. 283.

20 A. K. Rogerson, J. A. Aguilar, M. Nilsson and G. A. Morris, *Chem.Commun*., 2011, 47, 7063.

21 S. A. Willis, T. Stait-Gardner, A. S. Virk, R. Masuda, M. Zubkov, G. Zheng and W. S. Price*,* in *Modern NMR Techniques for Synthetic Chemistry* ed. Julie Fisher, CRC Press, 2014, Chapter 4. p. 125.

22 R. Evans, *Progress in NMR Spectroscopy*, 2020, 117, 33.

23. A. Macchioni, G. Ciancaleoni, C. Zuccaccia, D. Zuccaccia, *Chemical Society Reviews,* 2008, 37, 479.

24 C. A. Crutchfield and D. J. Harris, *J. Magn. Reson.,* 2007, 185, 179.

25 F. M. Arrabal, P. Ona-Burgos and I. Fernandez, *Polym. Chem.***,** 2016, **7**, 4326.

26 L. Castanar, G. Dal Poggetto, A. A. Colbourne, M. Nilsson and G. A. Morris, *Magn. Reson. Chem*., 2018, 56, 546.

27 R. Evans, G. Dal Poggetto, M. Nilsson and G. A. Morris, *Anal. Chem*., 2018, 90, 3987.

28 J. Reuben in *Nuclear Magnetic Resonance Shift Reagents*, ed. E. Sievers, Academic Press, Inc. London, 1973. p. 341.

29 E. J. Cabrita, S. Berger, P. Bräuer, J. Kärger, *J. Magn. Reson*., 2002, 157, 124.

30 T. Brand, E. J. Cabrita, S. Berger *Prog. NMR Spectrosc*., 2005, 46, 159.

31 D. J. Wijesekera, T. Stait-Gardner, A. Gupta, J. Chen, G. Zheng, A. M. Torres and W. S. Price, *Concepts in Magnetic Resonance Part* A, 2019, 47A, 21468.

32 W. Price, *NMR Studies of Translational Motion,* Cambridge University Press, Cambridge*,* 2009.

33 J. A. Peters, J. Huskens, D. J. Raber, *Progress in NMR Spectrosc.,* 1996, 28, 283.

34 D. S. Dyer, J. A. S. Cunningham, J. J. Brooks, R. E. Sievers and R. E. Rondeau, in *Nuclear Magnetic Resonance Shift Reagents*, ed. E. Sievers, Academic Press, Inc. London, 1973. p. 21.

35 E. O. Stejskal and T. E. Tanner *J. Chem. Phys*., 1965, 42, 288.

36 A. Chen, C. S. Johnson, M. Lin and M. J. Shapiro, *J. Am. Chem. Soc*., 1998, 120, 9094.

37 P. S. Pregosin, *Progress. NMR Spectrosc*., 2006, 49, 261.

38 I. Swan, M. Reid, P. W. A. Howe, M. A. Connell, M. Nilsson, M. A. Moore and G. A. Morris *J. Magn. Reson*., 2015, 252, 120.

39 T. Stait-Gardner, P. G. A. Kumolar and W. S. Price, *Chem. Phys. Letters*, 2008, 462, 331.

40 S. Berger and S. Braun, *200 and More NMR experiments*, Wiley-VCH Verlag, Weinheim, 2004.

41 S. Yu and L. Pu, *Tetrahedron*, 2015, 71, 745.

42 K. S. Salome and C. F. Tormena *Chem. Commun.,* 2019, 55, 8611.

43 V. I. Bakhmutov, *Practical NMR Relaxation for Chemists*, John Wiley& Sons, Chichester, 2004.

44 D. S. Meckl and M.D. Zeidler, *M. Phys*., 1988, 63, 85.

45 T. C. Morrill (ed) *Lanthanide Shift Reagents in Stereochemical Analysis*, VCH Publishers, INC. New York, 1986.

46 R. E. Sievers (ed) *Nuclear Magnetic Resonance Shift Reagents*, Academic Press, Inc. London, 1973.

47 I. Bertini, C. Luchinat and G. Parigi, *Solution NMR of Paramagnetic Molecules,* Elsevier, Amsterdam, 2001.

48 G. Szalontai *Magn. Reson. Chem*., 2021, 1-10. DOI: 10.1002/mrc.5151

49 A. W. J. Poh, J. A. Aguilar, A. M. Kenwright, K. Mason and D. Parker, *Chemistry, a European Journal,* 2018, 24, 6170.